*SUPPORTING INFORMATION*

# Mixed-Monolayer-Protected $Au_{25}$ Clusters with Bulky Calix[4]arene Functionalities

Jukka Hassinen,[†] Petri Pulkkinen,[‡] Elina Kalenius,[§] Thalappil Pradeep,[⊥] Heikki Tenhu, [‡] Hannu Häkkinen[§,#] and Robin H. A. Ras*[,†]

† Department of Applied Physics, Aalto University (Helsinki University of Technology), Puumiehenkuja 2, FI-02150 Espoo, Finland
‡ Department of Chemistry, University of Helsinki, P.O. Box 55, 00014 Helsinki, Finland
§ Department of Chemistry and [#]Department of Physics, Nanoscience Center, University of Jyväskylä, P.O. Box 35, 40014 JYU, Finland
⊥ DST Unit of Nanoscience (DST UNS), Department of Chemistry, Indian Institute of Technology, Madras, Chennai 600 036, India

## Index

## Experimental methods and characterization techniques

### *Chemicals*

Tetrachloroauric(III) acid ($HAuCl_4 \cdot 3\ H_2O$, ≥ 99,9 %), tetraoctylammonium bromide (TOAB, 98 %), 1-butanethiol (BuSH, 99 %), sodium borohydride ($NaBH_4$, 99 %), chloroform-d ($CDCl_3$, >99,96 %), tetrahydrofuran (THF, ≥ 99,0 %), methanol (HPLC grade) were purchased from Sigma-Aldrich. Bio-Beads® S-X1 were purchased from Bio-Rad. All the chemicals were used as received without further purification. The water used in experiments was Milli-Q grade with a resistivity of 18.2 MΩ·cm. The thiol-modified calix[4]arene (25,26,27,28-tetrakis(4-mercapto-n-butoxy)calix[4]arene, shortly Calix-4SH) was synthesized as described in the following section.

### *Synthesis of thiol-modified calix[4]arene (25,26,27,28-tetrakis(4-mercapto-n-butoxy)calix[4]arene)*

Calix-4SH was synthesized as reported[1]. Dry dimethylformamide (190 ml) was placed into a flask and purged with nitrogen. Calix[4]arene-25,26,27,28-tetrol (9.43 mmol), dibromobutane (188.5 mmol) and NaH (56.6 mmol) were added into the flask. (Caution: NaH reacts violently with water!) The mixture was stirred for 20 min, after which the flask was heated to 80 °C. The reaction mixture was stirred under $N_2$ for five days.

The reaction was quenched with careful water addition and the mixture was extracted twice with chloroform. The organic phase was washed with distilled water twice and dried with anhydrous sodium sulfate. Organic phase was evaporated under high vacuum (3 mbar, 140 ºC) in order to remove volatile organic substances and the most of the DBB. The residue was purified using column chromatography (chloroform:hexane 75:25, Rf 80%.). The yield was 49%. $^1$H NMR (300 MHz, $CDCl_3$) 6.3 (12H, s), 4.1 (4H, d), 3.6 (8H, t), 3.2 (8H, t), 2.9 (4H, d), 1.7 (16H, m).

A part of the product (3.77 mmol) of previous synthesis phase was placed in a nitrogen purged flask containing 125 ml of dry DMF. Thiourea (76.1 mmol) was added and the mixture was stirred for 20 min, after which the flask was heated to 80 °C. The mixture was stirred under nitrogen for 12 hours and then, was quenched by pouring the mixture into NaOH solution (3.8 %, 580 ml). The reaction mixture was stirred for one hour and finally the pH was adjusted to 4–5 using HCl. Product was filtered, washed with water, dried in vacuum and further purified using column chromatography (chloroform, Rf 75%.) Yield: 70%. $^1$H-NMR (300 MHz, $CDCl_3$) 6.6 (12H, s), 4.4 (4H, d), 3.9 (8H, t), 3.2 (4H, d), 2.6 (8H, q), 2.0 (8H, m) 1.7 (8H, m), 1.4 (4H, t).

### *Synthesis of calixarene-modified $Au_{25}$ clusters*

The calixarene functionalized clusters were synthesized by slightly modifying a method proposed by Qian *et al.*[2] Tetrachloroauric(III) acid (40 mg) was dissolved in 7.5 ml THF and 65 mg of TOAB was added while stirring the solution. The color of the reaction mixture changed from yellow to orange when continuing the stirring for 15 min. In a separate vial, a mixture of 55 µl BuSH and a varying amount of Calix-4SH was prepared and dissolved into 500 µl THF. The molar amount of Calix-

4SH in the thiol mixtures was varied between 0-7.0 % of the amount of BuSH. The thiol mixture was rapidly added to the reaction mixture under vigorous stirring (1200 RPM). The stirring was continued for 2 h during which the solution turned colorless. After that, 39 mg $NaBH_4$ dissolved in 2.5 ml ice-cold water was rapidly added to the reaction solution under vigorous stirring and the stirring was continued until distinct $Au_{25}$ cluster core absorption features were observed (Figure S1). The size-focusing process lasted typically 18-27 hours, the time increasing with the amount of Calix-4SH in the reaction mixture. When preparing clusters without Calix-4SH ($Au_{25}(BuS)_{18}$), the size-focusing period was reduced to five hours. After the size-focusing period, the solvent was removed from the reaction mixture by rotary vacuum evaporation and majority of excess thiols and TOABr was removed by centrifugal washing with methanol (4 times, 3000 RCF). Subsequently, the product was dissolved to THF and the white insoluble matter consisting most likely of Au(I)-thiolates was removed by centrifugation. The clusters in THF were further purified by size-exclusion chromatography. In the case of $Au_{25}(BuS)_{18}$, methanol:water mixture (3:1 v/v) was used in centrifugal washing.

### *Size-exclusion chromatography*

Bio-Beads® S-X1 (200-400 Mesh) was used as the stationary phase for size exclusion chromatography (SEC) as suggested in a recent work[3]. Briefly, nine grams of beads were swollen overnight in 90 ml THF and loaded in a column equipped with a glass frit. The beads were washed with several bed volumes of THF until a constant bed height (40 cm) was reached. The cluster samples were dissolved into 200 µl THF and eluted at 0.5–1 ml/min. The product was collected in 1 ml fractions which were analyzed by absorption spectroscopy. After combining fractions with $Au_{25}$ clusters, the solvent was evaporated and product washed twice with methanol. The solid powder was dissolved in THF and oxygen was removed by bubbling nitrogen through the solution. The product was stored at 4 °C.

### *UV-visible absorption spectroscopy*

Absorption spectra were recorded in UV–visible range with PerkinElmer Lambda 950 UV/Vis/NIR absorption spectrophotometer. Spectra were recorded in high quality quartz cells with 10 mm path length.

### *Fourier transform infrared spectroscopy*

Transmission spectra were recorded with Thermo Nicolet Avatar 380 FT-IR spectrometer using a Thermo Scientific Smart Orbit attenuated total reflection (ATR) accessory with a type II diamond tungsten carbide crystal. The spectra were acquired by averaging 64 scans with 4 $cm^{-1}$ resolution. Cluster samples were drop-casted directly onto the ATR crystal from tetrahydrofuran and evaporated to dryness with nitrogen flow. Background spectrum (air) was acquired before measurements and a blank spectrum recorded with no sample was subtracted from the raw data to obtain final spectra of clusters.

### *Fluorescence spectroscopy*

Fluorescence spectra of cluster solutions were recorded using a QuantaMaster 40 spectrofluorometer from Photon Technology International. A double excitation monochromator was used in the measurements to decrease the stray light level and the slits in excitation and emission monochromators were set to 5 nm. Fluorescence spectra were recorded using standard 90° measurement geometry and no filters in excitation or emission channel. The fluorescence spectra were corrected by subtracting a blank solvent background and by using instrument's excitation and emission corrections provided by the manufacturer.

### *Quantum yield determination*

The quantum yields ($\Phi_f$) of the clusters were measured by comparing the integrated emission intensities of cluster samples in THF to a known reference fluorophore 4-(Dicyanomethylene)-2-methyl-6-(4-dimethylaminostyryl)-4H-pyran (DCM) in ethanol ($\Phi_f$ = 0.435).[4] The absorbances ($A_x$) at the excitation wavelength ($\lambda_{ex}$ = 440 nm) were adjusted to approximately 0.1 when determining quantum yields. Quantum yields were calculated according to equations 1 and 2, where the integrated emission intensities $F^x$, absorption factors $f_x$ and refractive indices of sample (S) and reference fluorophore (R) are taken into account.

$$\Phi_f^S = \frac{f_R(\lambda_{ex})}{f_S(\lambda_{ex})} \frac{\int_{\lambda_{em}} F^S(\lambda_{em})}{\int_{\lambda_{em}} F^R(\lambda_{em})} \frac{n_S^2}{n_R^2} \Phi_f^R \quad (1)$$

$$f_x(\lambda_{ex}) = 1 - 10^{-A_x(\lambda_{ex})} \quad (2)$$

### *Electrospray ionization mass spectrometry*

The mass spectrometric experiments were performed with a QSTAR Elite ESI-Q-TOF mass spectrometer equipped with an API 200 TurboIonSpray ESI source from AB Sciex (former MDS Sciex) in Concord, Ontario (Canada). The samples for positive polarization experiments were prepared by diluting THF stock solutions with THF/MeOH 7:1 (*v/v*) where CsOAc was added to enhance the ionization. The final concentration of clusters in each sample solution was ~ 30 µM. The sample solutions for negative polarization experiments were prepared without CsOAc addition by diluting THF stock solutions with THF to give final sample concentration of ~ 40 µM. The samples were injected into the ESI source with a flow rate of 5 µl/min. The parameters were optimized to get maximum abundance of the ions under study. Room-temperature nitrogen was used as nebulization (10 psi ESI- and 35 psi ESI+) and as curtain gas (18 psi). The ion-source voltages of 5.5 kV for capillary, 50 V for the oriface plate (declustering potential), 10 V as potential difference between skimmer and pre-quadrupole, and between 250 V for the potential difference between the focusing ring and pre-quadrupole were used on positive polarization experiments (in negative polarization experiments the corresponding voltages were -4.5 kV, -20 V, -10 V and -250 V). Accumulation delay of 2 s, ion release delay of 6 ms and ion release width of 5 ms were used. Each spectrum was an average of spectra collected within 2 to 5 min, each of these containing 20 individual scans that were averaged before being sent from the instrument to data system. The measurement and data handling was accomplished with Analyst® QS 2.0

Software. Mass spectra were externally calibrated by using tetramethylated C2-resorcarene dendrimer (C2G3, compound **8**)[5]. The monoisotopic resolution was not always obtained, but the charge states of the ions were determined by characteristic $Cs^+$ mass differences and by comparison of the peak shape to shape of theoretic isotopic distributions. The compositions of the ions were finally verified by comparing experimental *m/z* values with the theoretical ones. The n(Calix-4S)/n(BuS) values were calculated based on the intensities of the peaks of different compositions in ESI-MS spectra.

### *Nuclear magnetic resonance spectroscopy*

Nuclear magnetic resonance (NMR) analyses were performed with Bruker Avance III spectrometer operating at 400 MHz. Typically, 1-2 mg of clusters dissolved in 600 µl $CDCl_3$ was used in analyses. For the analysis of mixed monolayer compositions, Iodine Death reaction was utilized. After measuring $^1$H-NMR spectra of clusters, a 20 µl drop of saturated iodine solution in $CDCl_3$ was added to the NMR tube and the tube was shaken for few minutes. After few hours, a deposit was detected at the bottom of the NMR-tube. $^1$H-NMR spectrum was recorded again and broadened signals were replaced with sharp signals from free ligands. The Calix:BuS ratios were calculated from spectra after Iodine Death reaction by integrating the Calix-4SH aromatic signal (6.6 ppm, 12H) and BuSH methylene signal next to the sulfur atom (2.7 ppm, 2H).

## Additional data

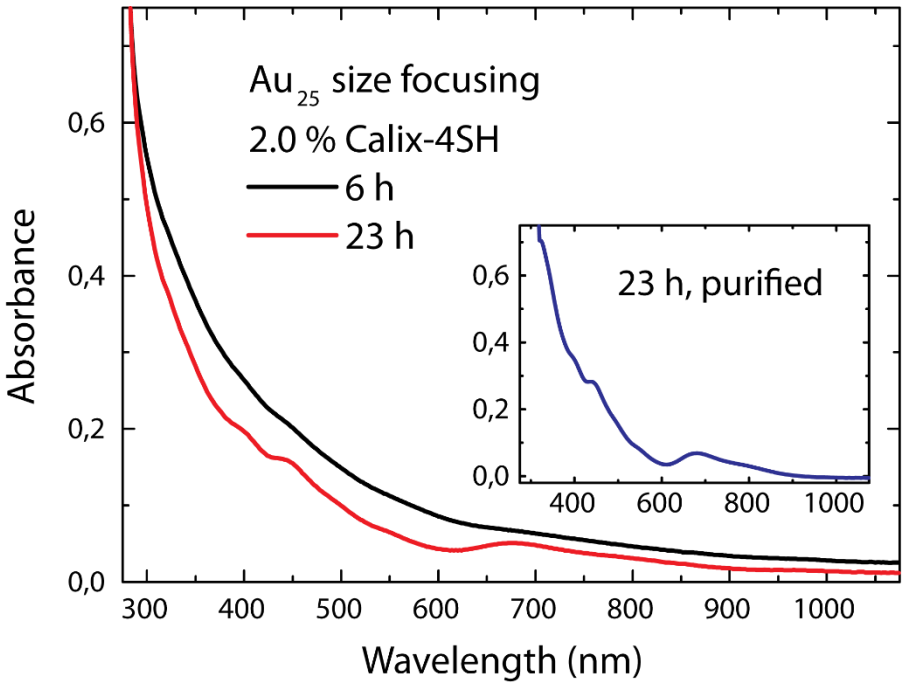


Figure S1. UV-vis absorption spectra of the reaction mixture during the size-focusing process of $Au_{25}$ clusters with 2.0 % Calix-4SH (Inset: purified clusters after size-focusing of 23 hours).

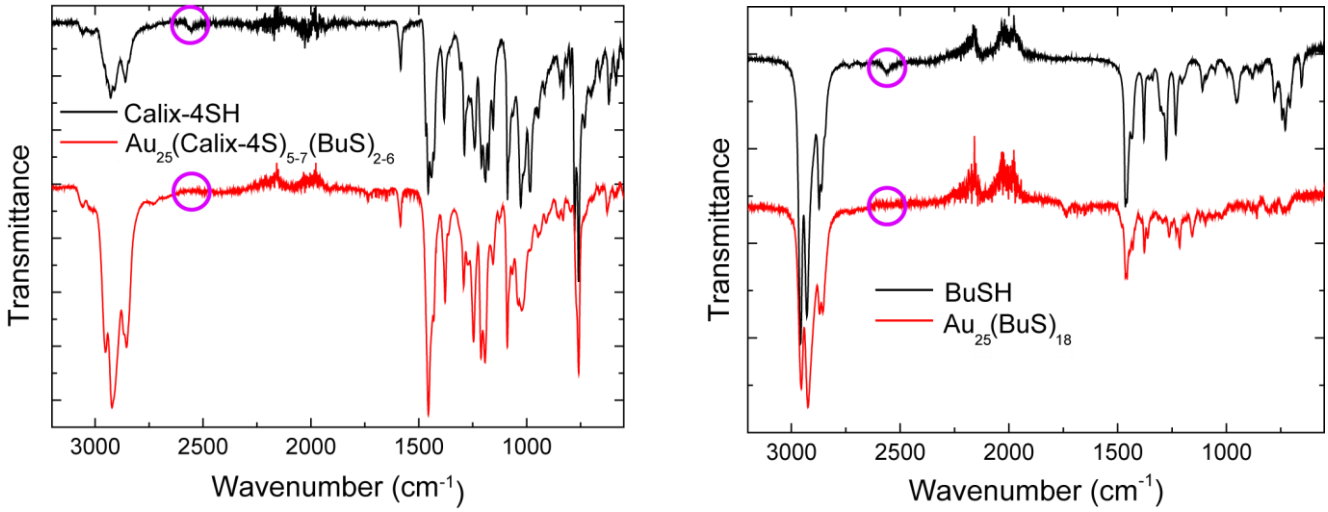


Figure S2. IR-spectra of Calix-4SH and calixarene-functionalized $Au_{25}$ clusters (left) as well as BuSH and $Au_{25}(BuS)_{18}$ (right). The band assigned to S-H stretching mode at 2560 $cm^{-1}$ disappears as ligands bind to clusters.

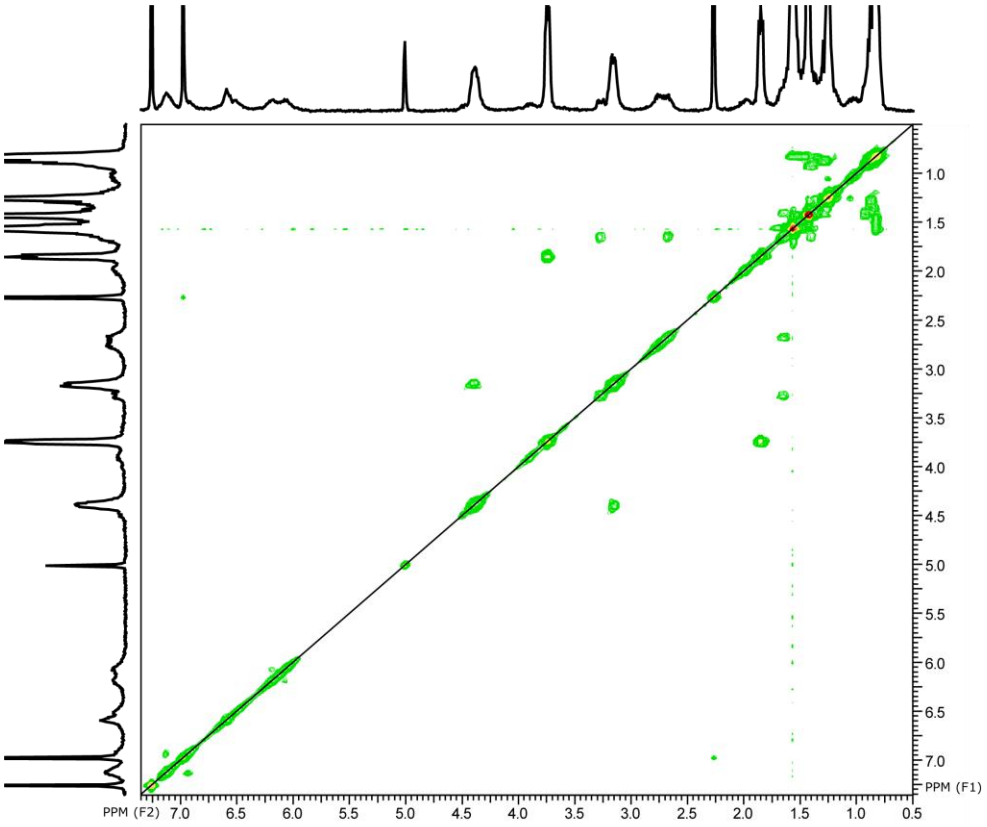


Figure S3. COSY spectrum of $Au_{25}$ clusters prepared by using 7.0 % Calix-4SH in the synthesis feed.

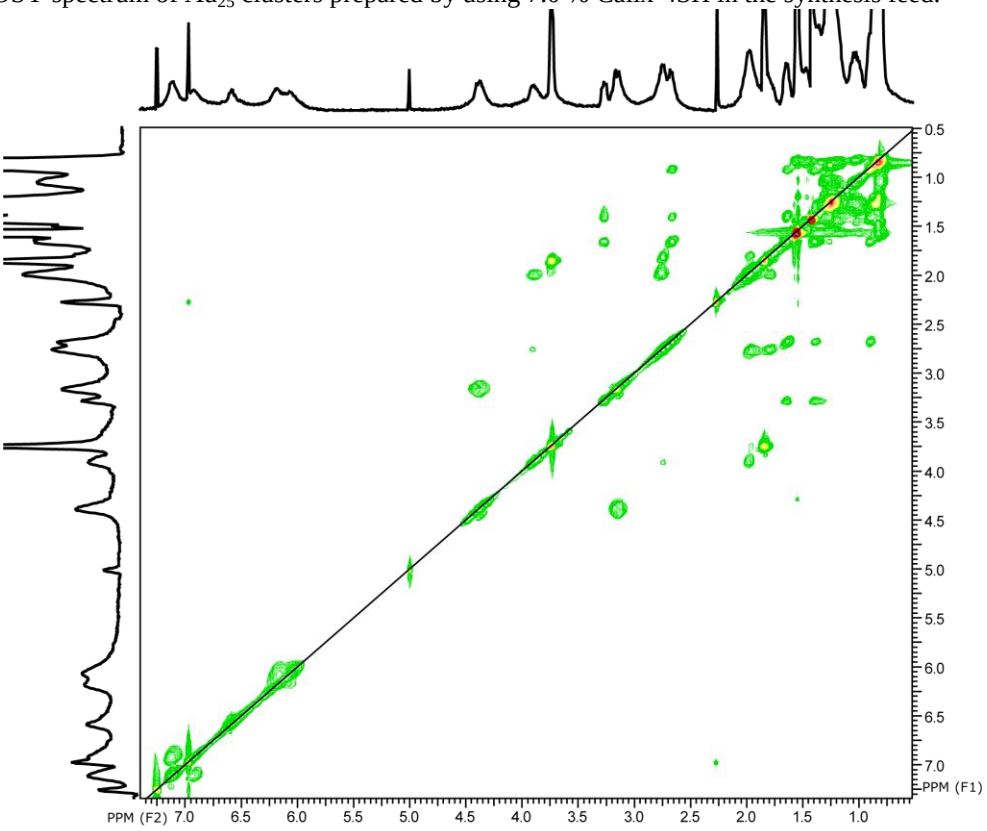


Figure S4. TOCSY spectrum of $Au_{25}$ clusters prepared by using 7.0 % Calix-4SH in the synthesis feed.

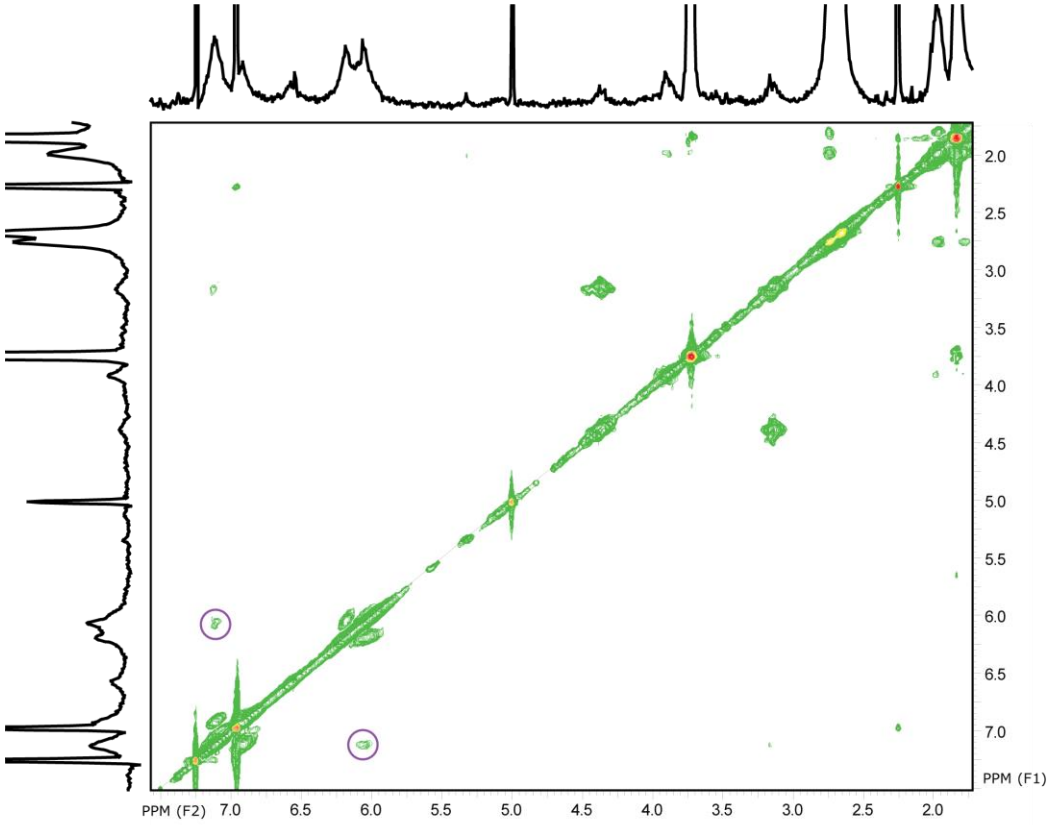


Figure S5. ROESY spectrum of $Au_{25}$ clusters prepared by using 7.0 % Calix-4SH in the synthesis feed. The coupling of the aromatic protons is highlighted with circles.

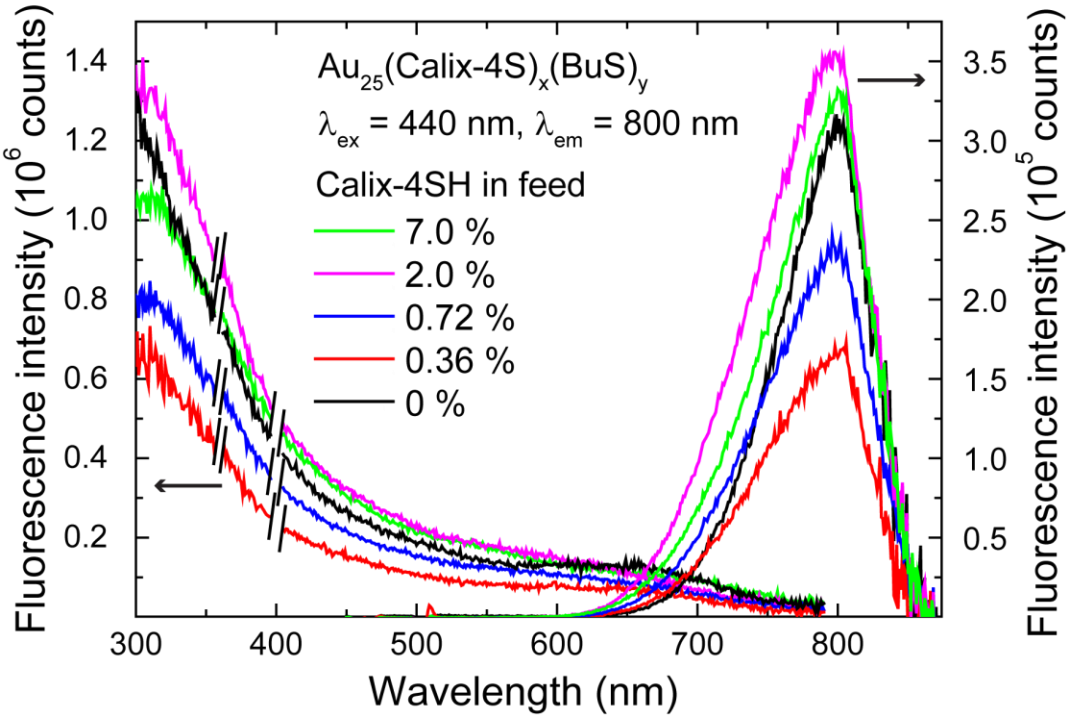


Figure S6. Fluorescence excitation and emission spectra of $Au_{25}(Calix\text{-}4S)_x(BuS)_y$ clusters. The second order excitation peak (400 nm) and THF raman peak (360 nm) have been omitted for clarity. It should be noted that the NIR emission can be limited by the detector at > 820 nm.

**Table S1. Fluorescence Quantum Yields of Cluster Products**

| Calix-4SH in feed (%) | Quantum yield (%) |
|---|---|
| 0 | 0.20 |
| 0.36 | 0.12 |
| 0.72 | 0.18 |
| 2.0 | 0.28 |
| 7.0 | 0.24 |

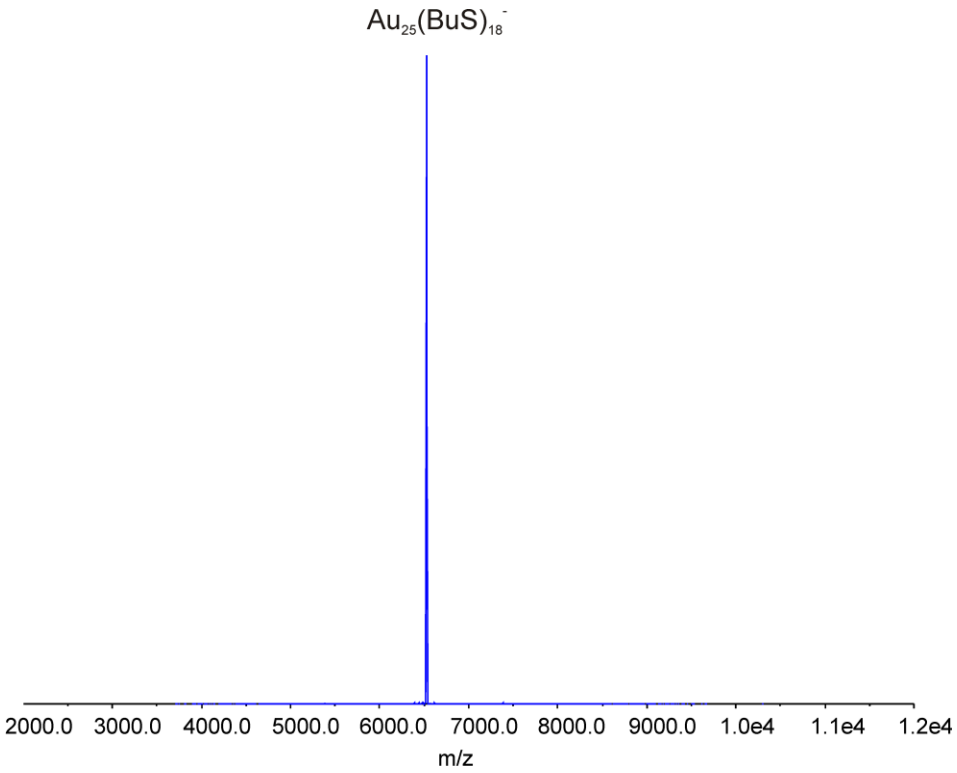


Figure S7. ESI(-)-TOF mass spectrum measured from sample obtained from 0.0 % Calix-4SH in the synthesis feed.

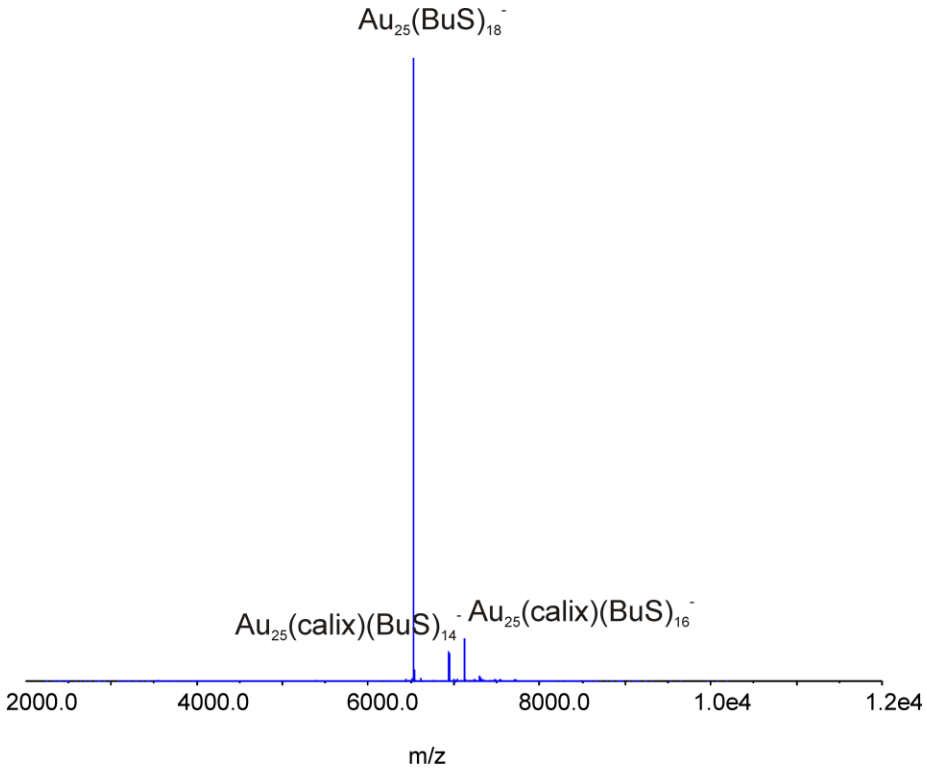


Figure S8. ESI(-)-TOF mass spectrum measured from sample obtained from 0.36 % Calix-4SH in the synthesis feed.

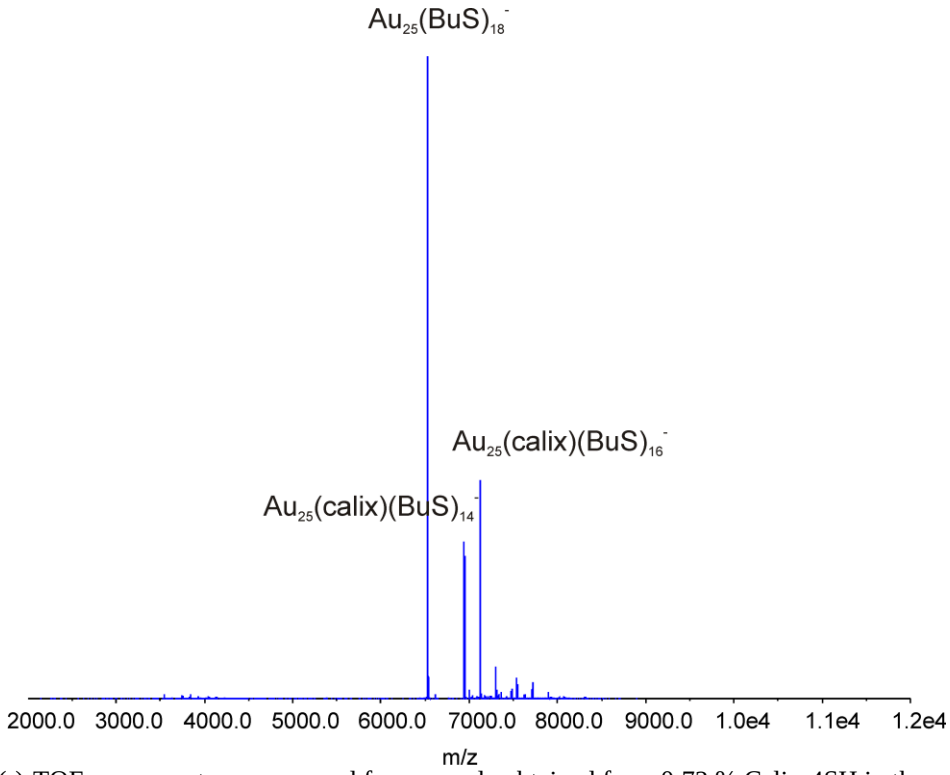


Figure S9. ESI(-)-TOF mass spectrum measured from sample obtained from 0.72 % Calix-4SH in the synthesis feed.

**Table S2. $Au_{25}(Calix\text{-}4S)_x(BuS)_y$ Clusters Observed in the ESI(+)-MS Spectra of Samples With Varying Calix-4SH Concentration in the Synthesis Feed and Interpretation of Ligands' Binding Modes**

| Cluster composition[a] | Calix-4S | | BuS bound to Au |
|---|---|---|---|
| | Tetradentate | Bidentate | |
| **0 % Calix-4SH in feed** | | | |
| $Au_{25}(BuS)_{18}$ | 0 | 0 | 18 |
| **0.36 % Calix-4SH in feed** | | | |
| $Au_{25}(BuS)_{18}$ | 0 | 0 | 18 |
| $Au_{25}(Calix\text{-}4S)(BuS)_{14}$ | 1 | 0 | 14 |
| $Au_{25}(Calix\text{-}4S)(BuS)_{16}$ | 0 | 1 | 16 |
| $Au_{25}(Calix\text{-}4S)_2(BuS)_{10}$ | 2 | 0 | 10 |
| $Au_{25}(Calix\text{-}4S)_2(BuS)_{12}$ | 1 | 1 | 12 |
| $Au_{25}(Calix\text{-}4S)_2(BuS)_{14}$ | 0 | 2 | 14 |
| **0.72 % Calix-4SH in feed** | | | |
| $Au_{25}(BuS)_{18}$ | 0 | 0 | 18 |
| $Au_{25}(Calix\text{-}4S)(BuS)_{14}$ | 1 | 0 | 14 |
| $Au_{25}(Calix\text{-}4S)(BuS)_{16}$ | 0 | 1 | 16 |
| $Au_{25}(Calix\text{-}4S)(BuS)_{18}$ | 0 | 1 | 16[b] |
| $Au_{25}(Calix\text{-}4S)_2(BuS)_{10}$ | 2 | 0 | 10 |
| $Au_{25}(Calix\text{-}4S)_2(BuS)_{12}$ | 1 | 1 | 12 |
| $Au_{25}(Calix\text{-}4S)_2(BuS)_{14}$ | 0 | 2 | 14 |
| $Au_{25}(Calix\text{-}4S)_2(BuS)_{16}$ | 0 | 2 | 14[b] |
| $Au_{25}(Calix\text{-}4S)_3(BuS)_6$ | 2 | 1 | 8 |
| $Au_{25}(Calix\text{-}4S)_3(BuS)_{10}$ | 1 | 2 | 10 |
| $Au_{25}(Calix\text{-}4S)_3(BuS)_{12}$ | 0 | 3 | 12 |
| $Au_{25}(Calix\text{-}4S)_3(BuS)_{14}$ | 0 | 3 | 12[b] |

| Cluster composition[a] | Calix-4S | | BuS bound to Au |
|---|---|---|---|
| | Tetradentate | Bidentate | |
| **2.0 % Calix-4SH in feed** | | | |
| $Au_{25}(Calix\text{-}4S)_2(BuS)_{12}$ | 1 | 1 | 12 |
| $Au_{25}(Calix\text{-}4S)_2(BuS)_{13}$[d] | 1 | 0 | 13 |
| $Au_{25}(Calix\text{-}4S)_2(BuS)_{14}$ | 0 | 2 | 14 |
| $Au_{25}(Calix\text{-}4S)_2(BuS)_{16}$ | 0 | 2 | 14[b] |
| $Au_{25}(Calix\text{-}4S)_3(BuS)_6$ | 2 | 1 | 8 |
| $Au_{25}(Calix\text{-}4S)_3(BuS)_{10}$ | 1 | 2 | 10 |
| $Au_{25}(Calix\text{-}4S)_3(BuS)_{12}$ | 0 | 3 | 12 |
| $Au_{25}(Calix\text{-}4S)_3(BuS)_{14}$ | 0 | 3 | 12[b] |
| $Au_{25}(Calix\text{-}4S)_4(BuS)_4$ | 3 | 1 | 4 |
| $Au_{25}(Calix\text{-}4S)_4(BuS)_6$ | 2 | 2 | 6 |
| $Au_{25}(Calix\text{-}4S)_4(BuS)_8$ | 1 | 3 | 8 |
| $Au_{25}(Calix\text{-}4S)_4(BuS)_{10}$ | 0 | 4 | 10 |
| $Au_{25}(Calix\text{-}4S)_4(BuS)_{12}$ | 0 | 4 | 10[b] |
| $Au_{25}(Calix\text{-}4S)_5(BuS)_4$ | 2 | 3 | 4 |
| $Au_{25}(Calix\text{-}4S)_5(BuS)_6$ | 1 | 4 | 6 |
| $Au_{25}(Calix\text{-}4S)_5(BuS)_8$ | 0 | 5 | 8 |
| $Au_{25}(Calix\text{-}4S)_5(BuS)_{10}$ | 0 | 5 | 8[b] |
| **7.0 % Calix-4SH in feed** | | | |
| $Au_{25}(Calix\text{-}4S)_5(BuS)_2$ | 3 | 2 | 2 |
| $Au_{25}(Calix\text{-}4S)_5(BuS)_4$ | 2 | 3 | 4 |
| $Au_{25}(Calix\text{-}4S)_5(BuS)_6$ | 1 | 4 | 6 |
| $Au_{25}(Calix\text{-}4S)_5(BuS)_8$ | 0 | 5 | 8 |
| $Au_{25}(Calix\text{-}4S)_5(BuS)_{10}$ | 0 | 5 | 8[b] |
| $Au_{25}(Calix\text{-}4S)_6(BuS)_2$ | 2 | 4 | 2 |
| $Au_{25}(Calix\text{-}4S)_6(BuS)_4$ | 1 | 5 | 4 |
| $Au_{25}(Calix\text{-}4S)_6(BuS)_5$[d] | 1 | 4 | 5 |
| $Au_{25}(Calix\text{-}4S)_6(BuS)_6$ | 0 | 6 | 6 |
| $Au_{25}(Calix\text{-}4S)_6(BuS)_8$ | 0 | 6 | 6[b] |
| $Au_{25}(Calix\text{-}4S)_7(BuS)_2$ | 1 | 6 | 2 |
| $Au_{25}(Calix\text{-}4S)_7(BuS)_4$ | 0 | 7 | 4 |
| $Au_{25}(Calix\text{-}4S)_7(BuS)_6$ | 0 | 7 | 4[b] |
| $Au_{25}(Calix\text{-}4S)_8(BuS)_4$ | 0 | 8 | 2[b] |
| $Au_{25}(Calix\text{-}4S)_8(BuS)_6$ | 0 | 8 | 2[c] |

a. Charge and adduct ions ($Cs^+$) are omitted
b. Two BuS are presumed to bind to Calix-4S with disulfide bridges
c. Four BuS are presumed to bind to Calix-4S with disulfide bridges
d. One Calix-4S is presumed to bind monodentately

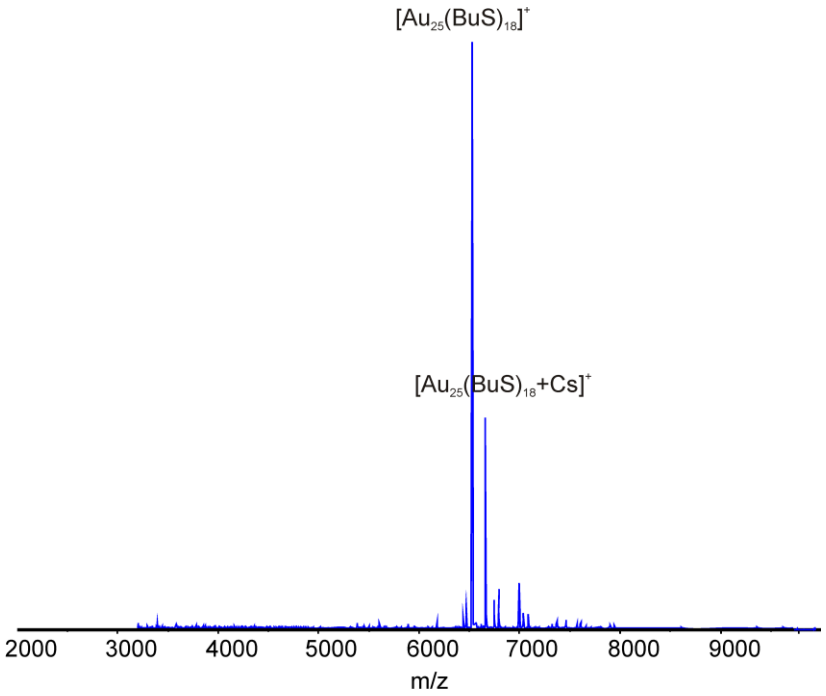


Figure S10. ESI(+)-TOF mass spectrum measured from sample obtained from 0.0 % Calix-4SH in the synthesis feed.

**Table S3**. **The Ions Observed in the ESI(+)-MS Spectrum Measured from 0.0 % Calix-4SH Feed: Theoretical and Experimental *m/z* values (Most Abundant) and Absolute Mass Accuracies**

| Ion | Ion Charge State | Core Charge | Composition | *m/z* (theor.) | *m/z* (exp.) | Mass Accuracy |
|---|---|---|---|---|---|---|
| $[Au_{25}(BuS)_{18}]^+$ | 1+ | 1+ | $C_{72}H_{162}S_{18}Au_{25}$ | 6528.9274 | 6528.8747 | 0.05 |
| $[Au_{25}(BuS)_{18} + Cs]^+$ | 1+ | 0 | $C_{72}H_{162}S_{18}Au_{25}Cs$ | 6661.8328 | 6661.8106 | 0.02 |
| $[Au_{25}(BuS)_{18} + Cs_2]^+$ | 1+ | 1- | $C_{72}H_{162}S_{18}Au_{25}Cs_2$ | 6794.7382 | 6794.6839 | 0.05 |
| $[Au_{25}(BuS)_{18} + TOA]^+$ | 1+ | 0 | $C_{104}H_{230}S_{18}Au_{25}N$ | 6995.4643 | 6995.4264 | 0.04 |

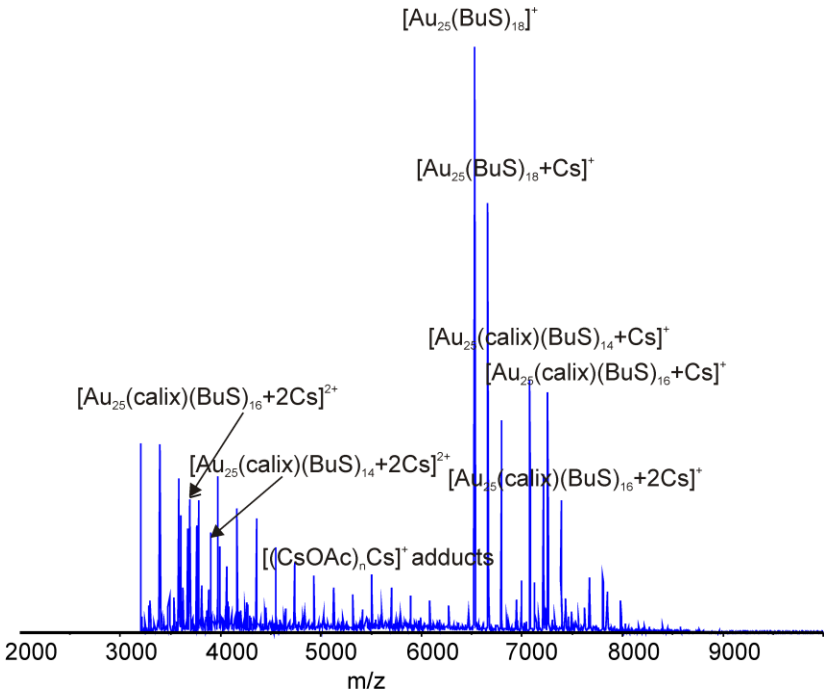


Figure S11. ESI(+)-TOF mass spectrum measured from sample obtained from 0.36 % Calix-4SH in the synthesis feed.

**Table S4. The Ions Observed in the ESI(+)-MS Spectrum Measured from 0.36 % Calix-4SH Feed: Theoretical and Experimental *m/z* Values (Most Abundant) and Absolute Mass Accuracies**

| Ion | Ion Charge State | Core Charge | Composition | *m/z* (theor.) | *m/z* (exp.) | Mass Accuracy |
|---|---|---|---|---|---|---|
| $[Au_{25}(BuS)_{18}]$ | 1+ | 1+ | $C_{72}H_{162}S_{18}Au_{25}$ | 6528.9274 | 6528.8747 | 0.05 |
| $[Au_{25}(BuS)_{18} + Cs]$ | 1+ | 0 | $C_{72}H_{162}S_{18}Au_{25}Cs$ | 6661.8328 | 6661.8106 | 0.02 |
| $[Au_{25}(BuS)_{18} + Cs_2]$ | 1+ | 1- | $C_{72}H_{162}S_{18}Au_{25}Cs_2$ | 6794.7382 | 6794.7096 | 0.03 |
| $[Au_{25}(calix)(BuS)_{14} +Cs]$ | 1+ | 0 | $C_{100}H_{178}O_4S_{18}Au_{25}Cs$ | 7077.9392 | 7077.8774 | 0.06 |
| $[Au_{25}(calix)(BuS)_{14} +Cs_2]$ | 1+ | 1- | $C_{100}H_{178}O_4S_{18}Au_{25}Cs_2$ | 7210.8447 | 7210.8037 | 0.04 |
| $[Au_{25}(calix)(BuS)_{16} +Cs]$ | 1+ | 0 | $C_{108}H_{196}O_4S_{20}Au_{25}Cs$ | 7256.0243 | 7255.9776 | 0.05 |
| $[Au_{25}(calix)(BuS)_{16} +Cs_2]$ | 1+ | 1- | $C_{108}H_{196}O_4S_{20}Au_{25}Cs_2$ | 7388.9297 | 7388.9334 | 0.00 |
| $[Au_{25}(calix)(BuS)_{14} +Cs_2]$ | 2+ | 0 | $C_{100}H_{178}O_4S_{18}Au_{25}Cs_2$ | 3605.4220 | 3605.4316 | -0.01 |
| $[Au_{25}(calix)(BuS)_{16} +Cs]$ | 2+ | 1+ | $C_{108}H_{196}O_4S_{20}Au_{25}Cs$ | 3628.0119 | 3628.0231 | -0.01 |
| $[Au_{25}(calix)(BuS)_{14} +Cs_2]$ | 2+ | 0 | $C_{100}H_{178}O_4S_{18}Au_{25}Cs_3$ | 3671.8748 | 3671.8745 | 0.00 |
| $[Au_{25}(calix)(BuS)_{16} +Cs_2]$ | 2+ | 0 | $C_{108}H_{196}O_4S_{20}Au_{25}Cs_2$ | 3694.4646 | 3694.4735 | -0.01 |
| $[Au_{25}(calix)(BuS)_{16} +Cs_3]$ | 2+ | 1- | $C_{108}H_{196}O_4S_{20}Au_{25}Cs_3$ | 3760.9173 | 3760.9473 | -0.03 |
| $[Au_{25}(calix)_2(BuS)_{10} +Cs_2]$ | 2+ | 0 | $C_{128}H_{194}O_8S_{18}Au_{25}Cs2$ | 3813.4750 | 3813.5258 | -0.05 |
| $[Au_{25}(calix)_2(BuS)_{12} +Cs_2]$ | 2+ | 0 | $C_{136}H_{212}O_{20}S_{20}Au_{25}Cs_2$ | 3902.5175 | 3902.5188 | 0.00 |
| $[Au_{25}(calix)_2(BuS)_{12} +Cs_2]$ | 2+ | 0 | $C_{136}H_{212}O_{20}S_{20}Au_{25}Cs_2$ | 3968.9703 | 3969.0439 | -0.07 |
| $[Au_{25}(calix)_2(BuS)_{14} +Cs_2]$ | 2+ | 0 | $C_{144}H_{230}O_8S_{22}Au_{25}Cs_2$ | 3992.0603 | 3992.0604 | 0.00 |
| $[Au_{25}(calix)_2(BuS)_{14} +Cs_3]$ | 2+ | 1- | $C_{144}H_{230}O_8S_{22}Au_{25}Cs_3$ | 4058.5130 | 4058.4983 | 0.01 |

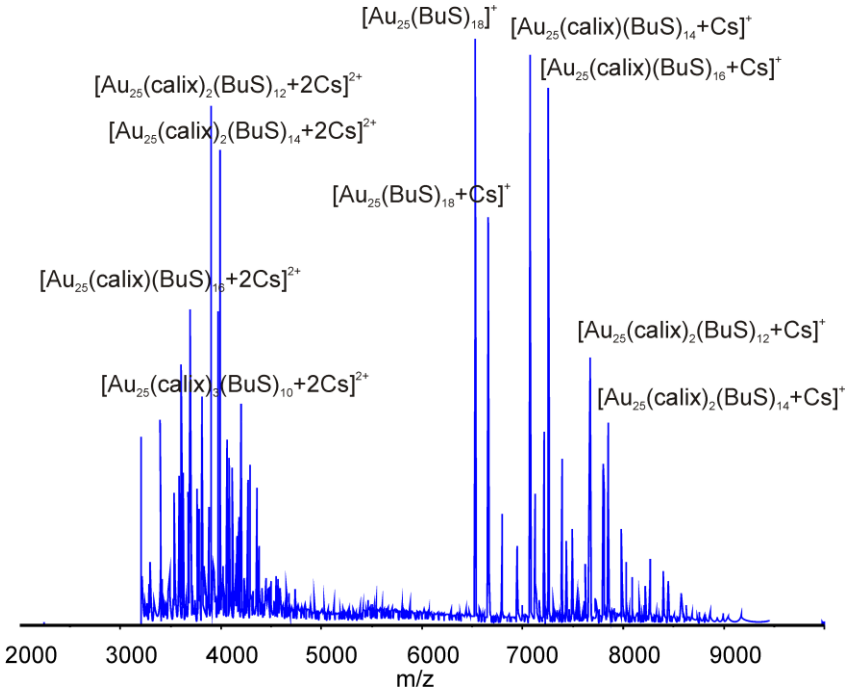


Figure S12. ESI(+)-TOF mass spectrum measured from sample obtained from 0.72 % Calix-4SH in the synthesis feed.

**Table S5. The Ions Observed in the ESI(+)-MS Spectrum Measured from 0.72 % Calix-4SH Feed: Theoretical and Experimental *m/z* Values (Most Abundant) and Absolute Mass Accuracies**

| Ion | Ion Charge State | Core Charge | Composition | *m/z* (theor.) | *m/z* (exp.) | Mass Accuracy |
|---|---|---|---|---|---|---|
| $[Au_{25}(BuS)_{18}]$ | 1+ | 1+ | $C_{72}H_{162}S_{18}Au_{25}$ | 6528.9274 | 6528.8747 | 0.05 |
| $[Au_{25}(BuS)_{18} + Cs]$ | 1+ | 0 | $C_{72}H_{162}S_{18}Au_{25}Cs$ | 6661.8328 | 6661.8106 | 0.02 |
| $[Au_{25}(BuS)_{18} + Cs_2]$ | 1+ | 1- | $C_{72}H_{162}S_{18}Au_{25}Cs_2$ | 6794.7382 | 6794.5836 | 0.15 |
| $[Au_{25}(calix)(BuS)_{14}]$ | 1+ | 1+ | $C_{100}H_{178}O_4S_{18}Au_{25}$ | 6945.0337 | 6944.9274 | 0.11 |
| $[Au_{25}(calix)(BuS)_{14} +Cs]$ | 1+ | 0 | $C_{100}H_{178}O_4S_{18}Au_{25}Cs$ | 7077.9392 | 7077.8774 | 0.06 |
| $[Au_{25}(calix)(BuS)_{16}]$ | 1+ | 1+ | $C_{108}H_{196}O_4S_{20}Au_{25}$ | 7123.1188 | 7123.1122 | 0.01 |
| $[Au_{25}(calix)(BuS)_{14} +Cs_2]$ | 1+ | 1- | $C_{100}H_{178}O_4S_{18}Au_{25}Cs_2$ | 7210.8447 | 7210.8037 | 0.04 |
| $[Au_{25}(calix)(BuS)_{16} +Cs]$ | 1+ | 0 | $C_{108}H_{196}O_4S_{20}Au_{25}Cs$ | 7256.0243 | 7255.9776 | 0.05 |
| $[Au_{25}(calix)(BuS)_{16} +Cs_2]$ | 1+ | 1- | $C_{108}H_{196}O_4S_{20}Au_{25}Cs_2$ | 7388.9297 | 7388.9334 | 0.00 |
| $[Au_{25}(calix)(BuS)_{18} +Cs]$ | 1+ | 0 | $C_{116}H_{214}O_4S_{22}Au_{25}Cs$ | 7434.1095 | 7434.0400 | 0.07 |
| $[Au_{25}(calix)_2(BuS)_{10} + Cs]$ | 1+ | 0 | $C_{128}H_{194}O_8S_{18}Au_{25}Cs$ | 7494.0453 | 7493.9500 | 0.10 |
| $[Au_{25}(calix)_2(BuS)_{10} +Cs_2]$ | 1+ | 1- | $C_{128}H_{194}O_8S_{18}Au_{25}Cs_2$ | 7626.9506 | 7626.9038 | 0.05 |
| $[Au_{25}(calix)_2(BuS)_{12} +Cs]$ | 1+ | 0 | $C_{136}H_{212}O_8S_{20}Au_{25}Cs$ | 7672.1302 | 7672.2019 | -0.07 |
| $[Au_{25}(calix)_2(BuS)_{12} +Cs_2]$ | 1+ | 1- | $C_{136}H_{212}O_8S_{20}Au_{25}Cs_2$ | 7805.0356 | 7805.0594 | -0.02 |
| $[Au_{25}(calix)_2(BuS)_{14} +Cs]$ | 1+ | 0 | $C_{144}H_{230}O_8S_{22}Au_{25}Cs$ | 7851.2157 | 7851.2176 | 0.00 |
| $[Au_{25}(calix)_2(BuS)_{14} +Cs_2]$ | 1+ | 1- | $C_{144}H_{230}O_8S_{22}Au_{25}Cs_2$ | 7984.1211 | 7984.0894 | 0.03 |
| $[Au_{25}(calix)_2(BuS)_{16} +Cs]$ | 1+ | 0 | $C_{152}H_{248}O_8S_{24}Au_{25}Cs$ | 8029.3006 | 8029.2488 | 0.05 |

| | | | | | | |
|---|---|---|---|---|---|---|
| $[Au_{25}(calix)_3(BuS)_8 + Cs]$ | 1+ | 0 | $C_{164}H_{228}O_{12}S_{20}Au_{25}Cs$ | 8089.2064 | 8089.1204 | 0.09 |
| $[Au_{25}(calix)_3(BuS)_{10} + Cs]$ | 1+ | 0 | $C_{172}H_{246}O_{12}S_{22}Au_{25}Cs$ | 8267.3214 | 8267.4367 | -0.12 |
| $[Au_{25}(calix)_3(BuS)_{10} + Cs_2]$ | 1+ | 1- | $C_{172}H_{246}O_{12}S_{22}Au_{25}Cs_2$ | 8400.2268 | 8400.1320 | 0.09 |
| $[Au_{25}(calix)_3(BuS)_{12} + Cs]$ | 1+ | 0 | $C_{180}H_{264}O_{12}S_{24}Au_{25}Cs$ | 8445.4063 | 8444.9200 | 0.49 |
| $[Au_{25}(calix)(BuS)_{14} + Cs]$ | 2+ | 1+ | $C_{100}H_{178}O_4S_{18}Au_{25}Cs$ | 3538.9693 | 3538.9736 | 0.00 |
| $[Au_{25}(calix)(BuS)_{14} + Cs_2]$ | 2+ | 0 | $C_{100}H_{178}O_4S_{18}Au_{25}Cs_2$ | 3605.4220 | 3605.4016 | 0.02 |
| $[Au_{25}(calix)(BuS)_{16} + Cs]$ | 2+ | 1+ | $C_{108}H_{196}O_4S_{20}Au_{25}Cs$ | 3628.0119 | 3628.0231 | -0.01 |
| $[Au_{25}(calix)(BuS)_{14} + Cs_2]$ | 2+ | 0 | $C_{100}H_{178}O_4S_{18}Au_{25}Cs_3$ | 3671.8748 | 3671.8745 | 0.00 |
| $[Au_{25}(calix)(BuS)_{16} + Cs_2]$ | 2+ | 0 | $C_{108}H_{196}O_4S_{20}Au_{25}Cs_2$ | 3694.4646 | 3694.4735 | -0.01 |
| $[Au_{25}(calix)(BuS)_{16} + Cs_3]$ | 2+ | 1- | $C_{108}H_{196}O_4S_{20}Au_{25}Cs_3$ | 3760.9173 | 3760.8314 | 0.09 |
| $[Au_{25}(calix)_2(BuS)_{10} + Cs_2]$ | 2+ | 0 | $C_{128}H_{194}O_8S_{18}Au_{25}Cs2$ | 3813.4750 | 3813.5258 | -0.05 |
| $[Au_{25}(calix)_2(BuS)_{12} + Cs_2]$ | 2+ | 0 | $C_{136}H_{212}O_{20}S_{20}Au_{25}Cs_2$ | 3902.5175 | 3902.9911 | -0.47 |
| $[Au_{25}(calix)_2(BuS)_{12} + Cs_2]$ | 2+ | 0 | $C_{136}H_{212}O_{20}S_{20}Au_{25}Cs_2$ | 3968.9703 | 3969.0439 | -0.07 |
| $[Au_{25}(calix)_2(BuS)_{14} + Cs_2]$ | 2+ | 0 | $C_{144}H_{230}O_8S_{22}Au_{25}Cs_2$ | 3992.0603 | 3992.0604 | 0.00 |
| $[Au_{25}(calix)_2(BuS)_{14} + Cs_3]$ | 2+ | 1- | $C_{144}H_{230}O_8S_{22}Au_{25}Cs_3$ | 4058.5130 | 4058.4983 | 0.01 |
| $[Au_{25}(calix)_2(BuS)_{16} + Cs_2]$ | 2+ | 0 | $C_{152}H_{248}O_8S_{24}Au_{25}Cs_2$ | 4081.1028 | 4081.1685 | -0.07 |
| $[Au_{25}(calix)_3(BuS)_8 + Cs_2]$ | 2+ | 0 | $C_{164}H_{228}O_8S_{24}Au_{25}Cs_2$ | 4111.0707 | 4110.5646 | 0.51 |
| $[Au_{25}(calix)_2(BuS)_{18} + Cs_2]$ | 2+ | 0 | $C_{160}H_{266}O_8S_{24}Au_{25}Cs_2$ | 4170.6449 | 4170.6498 | 0.00 |
| $[Au_{25}(calix)_3(BuS)_8 + Cs_3]$ | 2+ | 1- | $C_{164}H_{228}O_8S_{24}Au_{25}Cs_3$ | 4177.5234 | 4177.6498 | -0.13 |
| $[Au_{25}(calix)_3(BuS)_{10} + Cs_2]$ | 2+ | 0 | $C_{172}H_{246}O_{12}S_{22}Au_{25}Cs_2$ | 4200.1131 | 4200.1209 | -0.01 |
| $[Au_{25}(calix)_3(BuS)_{12} + Cs_2]$ | 2+ | 0 | $C_{180}H_{264}O_{12}S_{24}Au_{25}Cs_2$ | 4289.1557 | 4289.2803 | -0.12 |
| $[Au_{25}(calix)_3(BuS)_{12} + Cs_3]$ | 2+ | 1- | $C_{180}H_{264}O_{12}S_{24}Au_{25}Cs_3$ | 4355.6083 | 4355.1426 | 0.47 |
| $[Au_{25}(calix)_3(BuS)_{14} + Cs_2]$ | 2+ | 0 | $C_{180}H_{264}O_{12}S_{24}Au_{25}Cs_2$ | 4378.6980 | 4378.2505 | 0.45 |

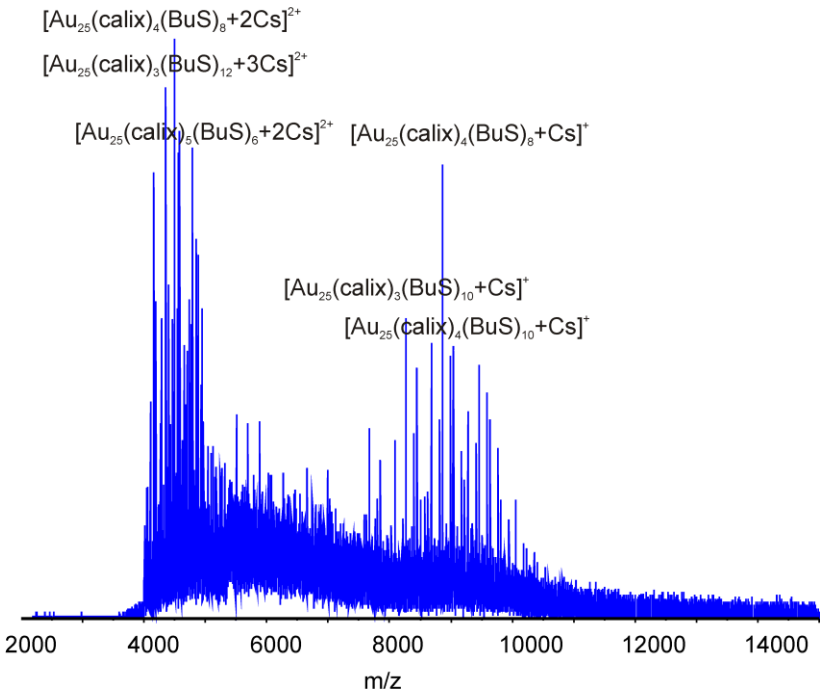


Figure S13. ESI(+)-TOF mass spectrum measured from sample obtained from 2.0 % Calix-4SH in the synthesis feed.

**Table S6. The Ions Observed in the ESI(+)-MS Spectrum Measured from 2.0 % Calix-4SH Feed: Theoretical and Experimental *m/z* Values (Most Abundant) and Absolute Mass Accuracies**

| Ion | Ion Charge State | Core Charge | Composition | *m/z* (theor.) | *m/z* (exp.) | Mass Accuracy |
|---|---|---|---|---|---|---|
| $[Au_{25}(calix)_2(BuS)_{12}+Cs]$ | 1+ | 0 | $C_{136}H_{212}O_8S_{20}Au_{25}Cs$ | 7672.1302 | 7672.8548 | -0.72 |
| $[Au_{25}(calix)_2(BuS)_{13}+Cs]$ | 1+ | 0 | $C_{140}H_{221}O_8S_{21}Au_{25}Cs$ | 7762.1731 | 7762.5171 | -0.34 |
| $[Au_{25}(calix)_2(BuS)_{12}+Cs_2]$ | 1+ | 1- | $C_{136}H_{212}O_8S_{20}Au_{25}Cs_2$ | 7805.0356 | 7805.8736 | -0.84 |
| $[Au_{25}(calix)_2(BuS)_{14}+Cs]$ | 1+ | 0 | $C_{144}H_{230}O_8S_{22}Au_{25}Cs$ | 7851.2157 | 7851.5278 | -0.31 |
| $[Au_{25}(calix)_2(BuS)_{14}+Cs_2]$ | 1+ | 1- | $C_{144}H_{230}O_8S_{22}Au_{25}Cs_2$ | 7984.1211 | 7983.2086 | 0.91 |
| $[Au_{25}(calix)_2(BuS)_{16}+Cs]$ | 1+ | 0 | $C_{152}H_{248}O_8S_{24}Au_{25}Cs$ | 8029.3006 | 8030.0553 | -0.75 |
| $[Au_{25}(calix)_3(BuS)_8+Cs]$ | 1+ | 0 | $C_{164}H_{228}O_{12}S_{20}Au_{25}Cs$ | 8089.2364 | 8089.6137 | -0.38 |
| $[Au_{25}(calix)_3(BuS)_{10}+Cs]$ | 1+ | 0 | $C_{172}H_{246}O_{12}S_{22}Au_{25}Cs$ | 8267.3214 | 8267.7189 | -0.40 |
| $[Au_{25}(calix)_3(BuS)_{10}+Cs_2]$ | 1+ | 1- | $C_{172}H_{246}O_{12}S_{22}Au_{25}Cs_2$ | 8400.2268 | 8400.5783 | -0.35 |
| $[Au_{25}(calix)_3(BuS)_{12}+Cs]$ | 1+ | 0 | $C_{180}H_{265}O_{12}S_{24}Au_{25}Cs$ | 8445.4063 | 8445.8527 | -0.45 |
| $[Au_{25}(calix)_4(BuS)_4+Cs]$ | 1+ | 0 | $C_{192}H_{244}O_{16}S_{20}Au_{25}Cs$ | 8505.3420 | 8504.6046 | 0.74 |
| $[Au_{25}(calix)_3(BuS)_{12}+Cs_2]$ | 1+ | 1- | $C_{180}H_{265}O_{12}S_{24}Au_{25}Cs_2$ | 8578.3119 | 8579.0796 | -0.77 |
| $[Au_{25}(calix)_4(BuS)_6+Cs]$ | 1+ | 0 | $C_{200}H_{262}O_{16}S_{22}Au_{25}Cs$ | 8684.4269 | 8683.9105 | 0.52 |
| $[Au_{25}(calix)_4(BuS)_6+Cs_2]$ | 1+ | 1- | $C_{200}H_{262}O_{16}S_{22}Au_{25}Cs_2$ | 8817.3325 | 8816.8649 | 0.47 |
| $[Au_{25}(calix)_4(BuS)_8+Cs]$ | 1+ | 0 | $C_{208}H_{280}O_{16}S_{24}Au_{25}Cs$ | 8862.5119 | 8861.8226 | 0.69 |
| $[Au_{25}(calix)_4(BuS)_8+Cs_2]$ | 1+ | 1- | $C_{208}H_{280}O_{16}S_{24}Au_{25}Cs_2$ | 8995.4175 | 8995.5890 | -0.17 |
| $[Au_{25}(calix)_4(BuS)_{10}+Cs]$ | 1+ | 0 | $C_{216}H_{298}O_{16}S_{26}Au_{25}Cs$ | 9040.5970 | 9040.9995 | -0.40 |

| | | | | | | |
|---|---|---|---|---|---|---|
| $[Au_{25}(calix)_4(BuS)_{10}+Cs_2]$ | 1+ | 1- | $C_{216}H_{298}O_{16}S_{26}Au_{25}Cs_2$ | 9173.5022 | 9173.934 | -0.43 |
| $[Au_{25}(calix)_4(BuS)_{12}+Cs]$ | 1+ | 0 | $C_{224}H_{316}O_{16}S_{28}Au_{25}Cs$ | 9218.2856 | 9217.9771 | 0.31 |
| $[Au_{25}(calix)_5(BuS)_4+Cs]$ | 1+ | 0 | $C_{236}H_{296}O_{20}S_{24}Au_{25}Cs$ | 9278.6178 | 9278.1398 | 0.48 |
| $[Au_{25}(calix)_5(BuS)_4+Cs_2]$ | 1+ | 1- | $C_{236}H_{296}O_{20}S_{24}Au_{25}Cs_2$ | 9411.5233 | 9411.6998 | -0.18 |
| $[Au_{25}(calix)_5(BuS)_6+Cs]$ | 1+ | 0 | $C_{244}H_{314}O_{20}S_{26}Au_{25}Cs$ | 9456.2011 | 9456.1256 | 0.08 |
| $[Au_{25}(calix)_5(BuS)_6+Cs_2]$ | 1+ | 1- | $C_{244}H_{314}O_{20}S_{26}Au_{25}Cs_2$ | 9589.6083 | 9588.9201 | 0.69 |
| $[Au_{25}(calix)_5(BuS)_8+Cs]$ | 1+ | 0 | $C_{252}H_{332}O_{20}S_{28}Au_{25}Cs$ | 9635.7877 | 9635.0603 | 0.73 |
| $[Au_{25}(calix)_5(BuS)_8+Cs_2]$ | 1+ | 1- | $C_{252}H_{332}O_{20}S_{28}Au_{25}Cs_2$ | 9768.6933 | 9767.9801 | 0.71 |
| $[Au_{25}(calix)_5(BuS)_{10}+Cs]$ | 1+ | 0 | $C_{260}H_{350}O_{20}S_{30}Au_{25}Cs$ | 9813.8727 | 9813.1319 | 0.74 |
| $[Au_{25}(calix)_3(BuS)_8+Cs_2]$ | 2+ | 0 | $C_{164}H_{228}O_8S_{24}Au_{25}Cs_2$ | 4111.0707 | 4110.6945 | 0.38 |
| $[Au_{25}(calix)_3(BuS)_{10}+Cs_2]$ | 2+ | 0 | $C_{172}H_{246}O_{12}S_{22}Au_{25}Cs_2$ | 4200.1131 | 4200.2444 | -0.13 |
| $[Au_{25}(calix)_3(BuS)_{10}+Cs_3]$ | 2+ | 1- | $C_{172}H_{246}O_{12}S_{22}Au_{25}Cs_3$ | 4266.5658 | 4266.5276 | 0.04 |
| $[Au_{25}(calix)_3(BuS)_{12}+Cs_2]$ | 2+ | 0 | $C_{180}H_{264}O_{12}S_{24}Au_{25}Cs_2$ | 4289.1557 | 4289.1499 | 0.01 |
| $[Au_{25}(calix)_3(BuS)_{12}+Cs_3]$ | 2+ | 1- | $C_{180}H_{264}O_{12}S_{24}Au_{25}Cs_3$ | 4355.6083 | 4355.0056 | 0.60 |
| $[Au_{25}(calix)_4(BuS)_6+Cs_2]$ | 2+ | 0 | $C_{200}H_{262}O_{16}S_{22}Au_{25}Cs_2$ | 4408.6659 | 4408.0513 | 0.61 |
| $[Au_{25}(calix)_4(BuS)_6+Cs_3]$ | 2+ | 1- | $C_{200}H_{262}O_{16}S_{22}Au_{25}Cs_3$ | 4475.1187 | 4475.0630 | 0.06 |
| $[Au_{25}(calix)_4(BuS)_8+Cs_2]$ | 2+ | 0 | $C_{208}H_{280}O_{16}S_{24}Au_{25}Cs_2$ | 4497.7085 | 4497.2168 | 0.49 |
| $[Au_{25}(calix)_4(BuS)_8+Cs_3]$ | 2+ | 1- | $C_{208}H_{280}O_{16}S_{24}Au_{25}Cs_3$ | 4564.1611 | 4564.1341 | 0.03 |
| $[Au_{25}(calix)_4(BuS)_{10}+Cs_2]$ | 2+ | 0 | $C_{216}H_{298}O_{16}S_{26}Au_{25}Cs_2$ | 4586.7509 | 4586.7630 | -0.01 |
| $[Au_{25}(calix)_4(BuS)_{10}+Cs_3]$ | 2+ | 1- | $C_{216}H_{298}O_{16}S_{26}Au_{25}Cs_3$ | 4653.2037 | 4652.6646 | 0.54 |
| $[Au_{25}(calix)_4(BuS)_{12}+Cs_2]$ | 2+ | 0 | $C_{224}H_{316}O_{16}S_{28}Au_{25}Cs_2$ | 4675.7934 | 4675.3825 | 0.41 |
| $[Au_{25}(calix)_5(BuS)_4+Cs_2]$ | 2+ | 0 | $C_{236}H_{296}O_{20}S_{24}Au_{25}Cs_2$ | 4705.7613 | 4705.6725 | 0.09 |
| $[Au_{25}(calix)_5(BuS)_4+Cs_3]$ | 2+ | 1- | $C_{236}H_{296}O_{20}S_{24}Au_{25}Cs_3$ | 4772.2140 | 4772.5505 | -0.34 |
| $[Au_{25}(calix)_5(BuS)_6+Cs_2]$ | 2+ | 0 | $C_{244}H_{314}O_{20}S_{26}Au_{25}Cs_2$ | 4794.8039 | 4795.1661 | -0.36 |
| $[Au_{25}(calix)_5(BuS)_6+Cs_3]$ | 2+ | 1- | $C_{244}H_{314}O_{20}S_{26}Au_{25}Cs_3$ | 4861.2565 | 4861.0934 | 0.16 |
| $[Au_{25}(calix)_5(BuS)_8+Cs_2]$ | 2+ | 0 | $C_{252}H_{332}O_{20}S_{28}Au_{25}Cs_2$ | 4884.3464 | 4883.9176 | 0.43 |
| $[Au_{25}(calix)_5(BuS)_8+Cs_3]$ | 2+ | 1- | $C_{252}H_{332}O_{20}S_{28}Au_{25}Cs_3$ | 4950.7990 | 4950.5830 | 0.22 |
| $[Au_{25}(calix)_5(BuS)_{10}+Cs_2]$ | 2+ | 0 | $C_{260}H_{350}O_{20}S_{30}Au_{25}Cs_2$ | 4973.3887 | 4973.3496 | 0.04 |
| $[Au_{25}(calix)_5(BuS)_{10}+Cs_3]$ | 2+ | 1- | $C_{260}H_{350}O_{20}S_{30}Au_{25}Cs_3$ | 5039.8415 | 5039.6813 | 0.16 |

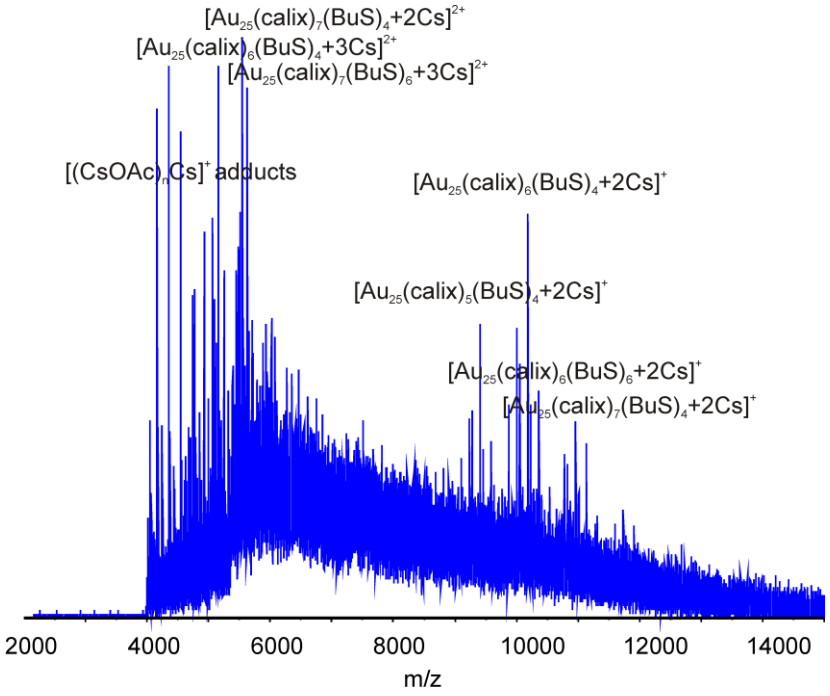


Figure S14. ESI(+)-TOF mass spectrum measured from sample obtained from 7.0 % Calix-4SH in the synthesis feed.

**Table S7. The Ions Observed in the ESI(+)-MS Spectrum Measured from 7.0 % Calix-4SH Feed: Theoretical and Experimental *m/z* Values (Most Abundant) and Absolute Mass Accuracies**

| Ion | Ion Charge State | Core Charge | Composition | *m/z* (theor.) | *m/z* (exp.) | Mass Accuracy |
|---|---|---|---|---|---|---|
| $[Au_{25}(calix)_5(BuS)_2 + Cs]$ | 1+ | 0 | $C_{228}H_{278}O_{20}S_{22}Au_{25}Cs$ | 9100.5330 | 9099.5010 | 1.03 |
| $[Au_{25}(calix)_5(BuS)_2 + Cs_2]$ | 1+ | 1- | $C_{228}H_{278}O_{20}S_{22}Au_{25}Cs_2$ | 9233.4382 | 9232.2867 | 1.15 |
| $[Au_{25}(calix)_5(BuS)_4 + Cs]$ | 1+ | 0 | $C_{236}H_{296}O_{20}S_{24}Au_{25}Cs$ | 9278.6178 | 9278.8680 | -0.25 |
| $[Au_{25}(calix)_5(BuS)_4 + Cs_2]$ | 1+ | 1- | $C_{236}H_{296}O_{20}S_{24}Au_{25}Cs_2$ | 9411.5233 | 9411.3165 | 0.21 |
| $[Au_{25}(calix)_5(BuS)_6 + Cs]$ | 1+ | 0 | $C_{244}H_{314}O_{20}S_{26}Au_{25}Cs$ | 9456.2011 | 9456.1256 | 0.08 |
| $[Au_{25}(calix)_5(BuS)_6 + Cs_2]$ | 1+ | 1- | $C_{244}H_{314}O_{20}S_{26}Au_{25}Cs_2$ | 9589.6083 | 9589.4738 | 0.13 |
| $[Au_{25}(calix)_6(BuS)_2 + Cs]$ | 1+ | 0 | $C_{272}H_{330}O_{24}S_{26}Au_{25}Cs$ | 9873.8088 | 9873.6423 | 0.17 |
| $[Au_{25}(calix)_6(BuS)_2 + Cs_2]$ | 1+ | 1- | $C_{272}H_{330}O_{24}S_{26}Au_{25}Cs_2$ | 10006.7141 | 10006.501 | 0.21 |
| $[Au_{25}(calix)_6(BuS)_4 + Cs]$ | 1+ | 0 | $C_{280}H_{348}O_{24}S_{28}Au_{25}Cs_1$ | 10051.8934 | 10052.273 | -0.38 |
| $[Au_{25}(calix)_6(BuS)_4 + Cs_2]$ | 1+ | 1- | $C_{280}H_{348}O_{24}S_{28}Au_{25}Cs_2$ | 10184.7989 | 10184.838 | -0.04 |
| $[Au_{25}(calix)_6(BuS)_6 + Cs]$ | 1+ | 0 | $C_{288}H_{366}O_{24}S_{30}Au_{25}Cs$ | 10229.9785 | 10231.819 | -1.84 |
| $[Au_{25}(calix)_6(BuS)_6 + Cs_2]$ | 1+ | 1- | $C_{288}H_{366}O_{24}S_{30}Au_{25}Cs_2$ | 10362.8838 | 10361.671 | 1.21 |
| $[Au_{25}(calix)_7(BuS)_2 + Cs_2]$ | 1+ | 1- | $C_{316}H_{382}O_{28}S_{30}Au_{25}Cs_2$ | 10779.9899 | 10780.946 | -0.96 |
| $[Au_{25}(calix)_7(BuS)_4 + Cs]$ | 1+ | 0 | $C_{324}H_{400}O_{28}S_{32}Au_{25}Cs$ | 10825.1692 | 10824.861 | 0.31 |
| $[Au_{25}(calix)_7(BuS)_4 + Cs_2]$ | 1+ | 1- | $C_{324}H_{400}O_{28}S_{32}Au_{25}Cs_2$ | 10958.0747 | 10957.698 | 0.38 |
| $[Au_{25}(calix)_7(BuS)_6 + Cs_2]$ | 1+ | 1- | $C_{332}H_{418}O_{28}S_{34}Au_{25}Cs_2$ | 11136.1596 | 11135.688 | 0.47 |
| $[Au_{25}(calix)_5(BuS)_2 + Cs_3]$ | 2+ | 1- | $C_{236}H_{296}O_{20}S_{24}Au_{25}Cs_3$ | 4683.1716 | 4683.0519 | 0.12 |

| | | | | | | |
|---|---|---|---|---|---|---|
| $[Au_{25}(calix)_5(BuS)_4+Cs_2]$ | 2+ | 0 | $C_{236}H_{296}O_{20}S_{24}Au_{25}Cs_2$ | 4705.7613 | 4705.1973 | 0.56 |
| $[Au_{25}(calix)_5(BuS)_4+Cs_3]$ | 2+ | 1- | $C_{236}H_{296}O_{20}S_{24}Au_{25}Cs_3$ | 4772.2140 | 4772.7306 | -0.52 |
| $[Au_{25}(calix)_5(BuS)_6+Cs_2]$ | 2+ | 0 | $C_{244}H_{314}O_{20}S_{26}Au_{25}Cs_2$ | 4794.8039 | 4795.0868 | -0.28 |
| $[Au_{25}(calix)_5(BuS)_6+Cs_3]$ | 2+ | 1- | $C_{244}H_{314}O_{20}S_{26}Au_{25}Cs_3$ | 4861.2565 | 4860.8874 | 0.37 |
| $[Au_{25}(calix)_5(BuS)_8+Cs_2]$ | 2+ | 0 | $C_{252}H_{332}O_{20}S_{28}Au_{25}Cs_2$ | 4884.3464 | 4884.3736 | -0.03 |
| $[Au_{25}(calix)_6(BuS)_2+Cs_2]$ | 2+ | 0 | $C_{272}H_{330}O_{24}S_{26}Au_{25}Cs_2$ | 5003.3568 | 5003.3221 | 0.03 |
| $[Au_{25}(calix)_6(BuS)_2+Cs_3]$ | 2+ | 1- | $C_{272}H_{330}O_{24}S_{26}Au_{25}Cs_3$ | 5069.8095 | 5069.647 | 0.16 |
| $[Au_{25}(calix)_6(BuS)_4+Cs_2]$ | 2+ | 0 | $C_{280}H_{348}O_{24}S_{28}Au_{25}Cs_2$ | 5092.3992 | 5092.4946 | -0.10 |
| $[Au_{25}(calix)_6(BuS)_4+Cs_3]$ | 2+ | 1- | $C_{280}H_{348}O_{24}S_{28}Au_{25}Cs_3$ | 5158.8519 | 5158.2616 | 0.59 |
| $[Au_{25}(calix)_6(BuS)_6+Cs_2]$ | 2+ | 0 | $C_{288}H_{366}O_{24}S_{30}Au_{25}Cs_2$ | 5181.4417 | 5180.8219 | 0.62 |
| $[Au_{25}(calix)_6(BuS)_5+Cs_3]$ | 2+ | 1- | $C_{284}H_{357}O_{24}S_{29}Au_{25}Cs_3$ | 5203.3732 | 5204.8419 | -1.47 |
| $[Au_{25}(calix)_6(BuS)_6+Cs_3]$ | 2+ | 1- | $C_{288}H_{366}O_{24}S_{30}Au_{25}Cs_3$ | 5247.8944 | 5248.3874 | -0.49 |
| $[Au_{25}(calix)_6(BuS)_6+Cs_4]$ | 2+ | 2- | $C_{288}H_{366}O_{24}S_{30}Au_{25}Cs_4$ | 5314.3471 | 5314.4613 | -0.11 |
| $[Au_{25}(calix)_6(BuS)_8+Cs_3]$ | 2+ | 1- | $C_{296}H_{384}O_{24}S_{32}Au_{25}Cs_3$ | 5337.4368 | 5337.9127 | -0.48 |
| $[Au_{25}(calix)_7(BuS)_4+Cs_2]$ | 2+ | 0 | $C_{324}H_{400}O_{28}S_{32}Au_{25}Cs_2$ | 5479.0371 | 5478.4458 | 0.59 |
| $[Au_{25}(calix)_7(BuS)_4+Cs_3]$ | 2+ | 0 | $C_{324}H_{400}O_{28}S_{32}Au_{25}Cs_3$ | 5545.4898 | 5545.1033 | 0.39 |
| $[Au_{25}(calix)_7(BuS)_6+Cs_2]$ | 2+ | 0 | $C_{332}H_{418}O_{28}S_{34}Au_{25}Cs_2$ | 5568.0795 | 5568.2112 | -0.13 |
| $[Au_{25}(calix)_7(BuS)_6+Cs_3]$ | 2+ | 1- | $C_{332}H_{418}O_{28}S_{34}Au_{25}Cs_3$ | 5634.5323 | 5634.4177 | 0.11 |
| $[Au_{25}(calix)_8(BuS)_4+Cs_3]$ | 2+ | 1- | $C_{368}H_{452}O_{32}S_{36}Au_{25}Cs_3$ | 5932.1276 | 5932.2377 | -0.11 |
| $[Au_{25}(calix)_8(BuS)_6+Cs_3]$ | 2+ | 1- | $C_{376}H_{470}O_{32}S_{38}Au_{25}Cs_3$ | 6021.1702 | 6021.0844 | 0.09 |

## References


(1) Ha, J.-M.; Katz, A.; Drapailo, A. B.; Kalchenko, V. I. *J. Phys. Chem. C* **2009**, *113*, 1137.
(2) Qian, H.; Liu, C.; Jin, R. *Science China* **2012**, *55*, 2359.
(3) Knoppe, S.; Michalet, S.; Bürgi, T. *J. Phys. Chem. C* **2013**, *117*, 15354.
(4) Rurack, K; Spieles, M. *Anal. Chem.* **2011**, *83*, 1232.
(5) Luostarinen, M.; Salorinne, K.; Lähteenmäki, H.; Mansikkamäki, H.; Schalley, C. A.; Nissinen, M.; Rissanen, R. *J. Incl. Phenom. Macrocycl. Chem.* **2007**, 58, 71.